Damage Evaluation of the Human Eye for Different Laser Sources–Connecting Ray Tracing and Finite Volume Calculations

Nico Heussner[2] and Wilhelm Stork[1, 2]
[1]Karlsruhe Institute of Technology/ITIV, Karlsruhe, Germany
[2]FZI Forschungszentrum Informatik/ESS, Karlsruhe, Germany
Email: {Wilhelm.Stork, Heussner}@kit.edu

***Abstract*—A tool chain is presented which allows an estimation of the danger a laser source can pose to the human eye. It makes use of a ray tracing approach to define the spot positions and diameters within the eye. This information is then used to calculate the temperature and likelihood of damage via Finite Volume Method (FVM) calculations. Therefore a previously developed computer model of the human eye is incorporated which allows to determine the thermal behaviour over time as well as tissue damage. The method is exemplarily demonstrated for a scanning laser device and the influence of the accommodation state on the ocular hazard is pointed out.**

***Index Terms*—damage evaluation, human eye, laser-tissue interaction, retinal damage, eye safety**

I. Introduction

With the growing number of applications, it becomes increasingly important to have an opportunity for fast and easy evaluation of laser devices concerning eye safety. Since the safety standards are quite complex, it is a difficult and time extensive task to evaluate the danger during the design process where parameters change very often [1] [2]. Therefore we present a system which enables the user to calculate the effects of the device to the human eye and therefore draw conclusions about the level of safety and how to improve it.

Our method employs calculations which are dependent on laser source properties, the distance between the source and the accommodation state of the eye lense. This is realized by a tool chain incorporating Matlab, Zemax, Ansys Fluent and Altair Hypermesh. The functionality is demonstrated for the case of scanning lasers which are e.g. used in the field of retinal imaging, environmental scanning or displays [3]-[5].

II. Material and Methods

The tool chain is visualized in Fig. 1 stepwise. It can be divided into two main sections which are described in the following:

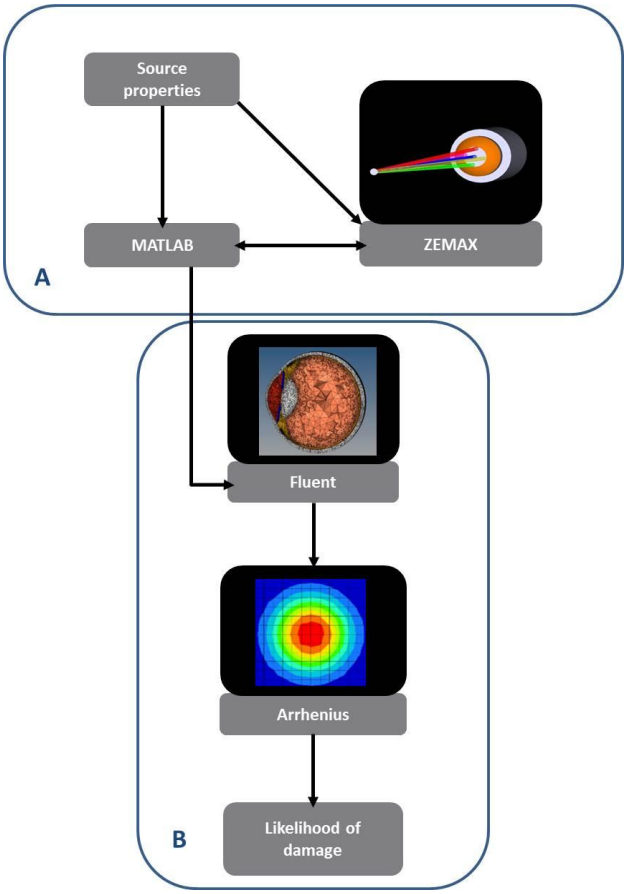

Figure 1. Tool chain

TABLE I. Source Properties A

Source type	Scanning laser (deflective mirror)
Wavelength	Visible
Spot diameter	1 mm
Ray convergence	Collimated
Maximum tilt angle	±1 °
Resolution / step size tilt angle	0.5 °

A. Raytracing (Matlab & Zemax)

Starting point of the calculations is the modeling of the laser source in Matlab and Zemax. In the case of a

Manuscript received July 25, 2014; revised December 2, 2014.

doi: 10.12720/jomb.4.6.475-479

scanning laser devices, the parameters are: The tilt angles in two dimensions (Matlab), the spot diameter (Zemax) and the convergence angle (Zemax). The laser power and the duration of each time step are not important at this stage and will be dealt with later on. The properties which were used are given in Table I.

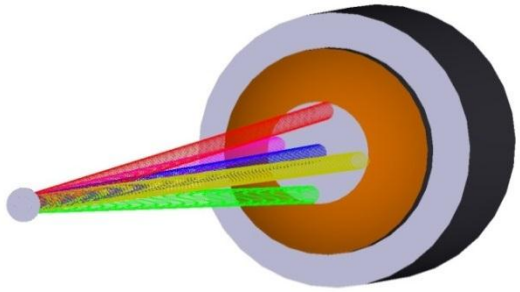

Figure 2. Zemax model of a scanning mirror (left) and a human eye (right)

This light source is then placed in front of a Zemax implementation of the Navarro eye model [6] which additionally includes the opportunity to change the accommodation state between an optical power of 59dpt (relaxed eye) and 71dpt (100mm viewing distance). The eye model and the scanning mirror are shown in Fig. 2, while Fig. 3 illustrates the path of the rays through the eye.

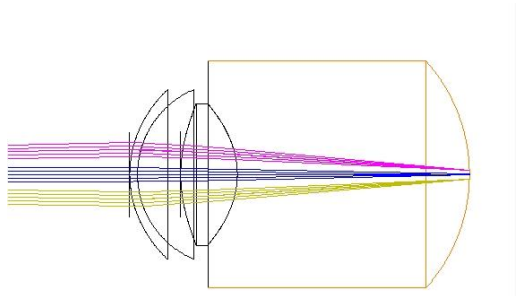

Figure 3. Different spot positions on the retina for different scanning angles of the mirror

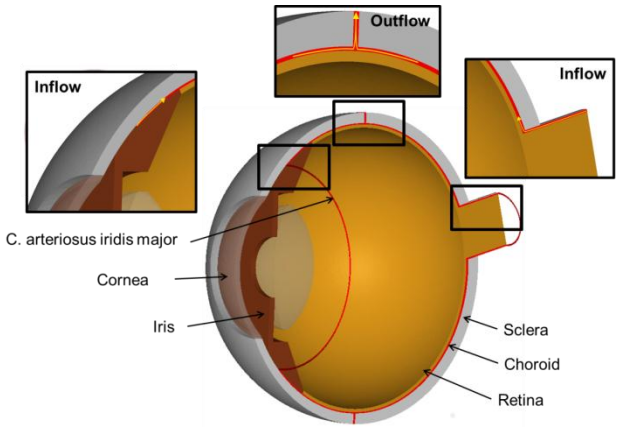

Figure 4. Perspective view of the eye model [8]

Matlab is responsible for controlling the input of the laser source (i.e. tilting the mirror in this case) and reading the spot positions and diameters at the different regions of the eye. We assume a distance mirror-eye of 100 mm which is the worst-case scenario for laser safety considerations [7]. Finally the positions and sizes of the spots are written into a data-file which is accessed by the FVM part of the tool chain.

B. FVM (Ansys Fluent & C++)

This part of the tool chain is based on our previous work [8]. in which a computer model of the human eye was established which can predict the temperatures and likelihood of damage during laser irradiation (Fig. 4).

Part *B* is reading the data-file from *A* via a so-called *user-defined-function (UDF)* Within the Ansys Fluent software. Thereby the illumination sequence is loaded into the *FVM* software. The time step size and the laser power are added at this point. For the presented device we used the parameters presented in Table II.

TABLE II. SOURCE PROPERTIES B

Source type	Scanning laser (deflective mirror)
Power	1 W
Time step size	10 µs

Within the visible wavelength regime we assume an absorption at the retinal pigment epithel of 51% and a lambert-beer distribution of the remaining energy in the choroidal layer with an absorption of μ_a = 270/cm [8]. The transmission behavior from the cornea to the retina is T = 30 % [9] [10]. Using these assumptions the energy applied to the eye is written cell by cell into the mesh (see [8] for details) and a time dependent temperature distribution is obtained. These temperatures are then further processed by a C++ program to calculate the Arrhenius integral which is a measure for tissue damage [11] [8].

III. RESULTS

A. Raytracing

If a scanning laser is entering the human eye the irradiation behaviour on the retina depends on the distance between the scanning mirror and the eye and the accomodation state of the eye [4] [12]. For a given distance of 100 mm Fig. 5 shows the spot movement on the retina for different accomodation states.

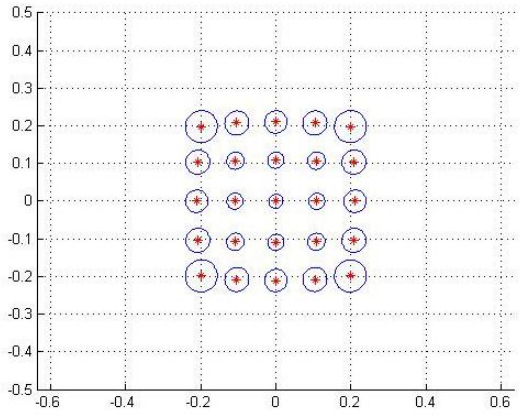

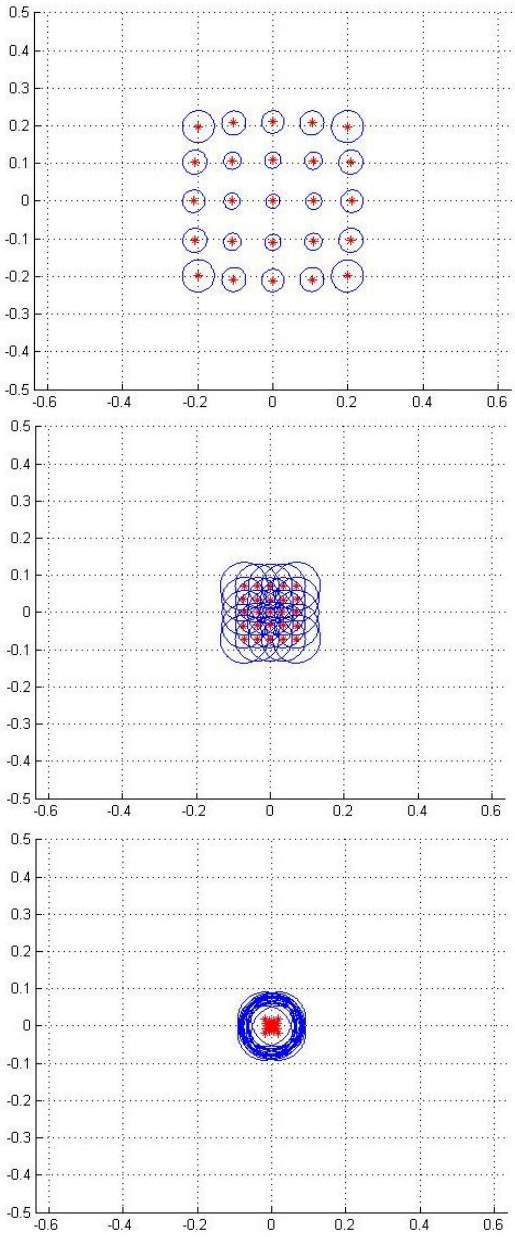

Figure 5. Retinal scanning vs. accomodation state (scaling in mm / optical power from top to bottom: 61dpt, 67dpt,71dpt)

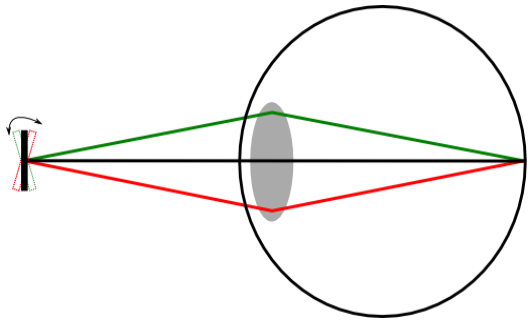

Figure 6. A scanning mirror acts as a quasi-point-source

Each red point corresponds with the center of a spot on the retina, the blue circles describe the respective spot diameters. It was assumed that each line scan started on the left hand side and moved to the right while the lines were scanned from top to bottom. As Fig. 5 indicates, the scanning range on the retina decreases with increasing accommodation until it almost forms a single spot. This "quasi-point-source" occurs, if the object distance and accmodation distance are equal (see Fig. 6 and [12]).

The spot information is then stored into a file which is further processed by the Finite Volume Method calculations described in the following chapter.

B. Finite Volume Method Calculations

Fig. 7-Fig. 9 depict the heating process of the retina for different accommodation states. 25 spots were used, each with an irradiation time of 10 µs. This means that e.g. 130 µs correspond with 13 spots being used (see Fig. 7) and 250 µs with the maximum number of spots which is 25. With an increasing optical power and therefore a decreasing accommodation distance, the overlap of the heatead areas increases until only one spot can be observed.

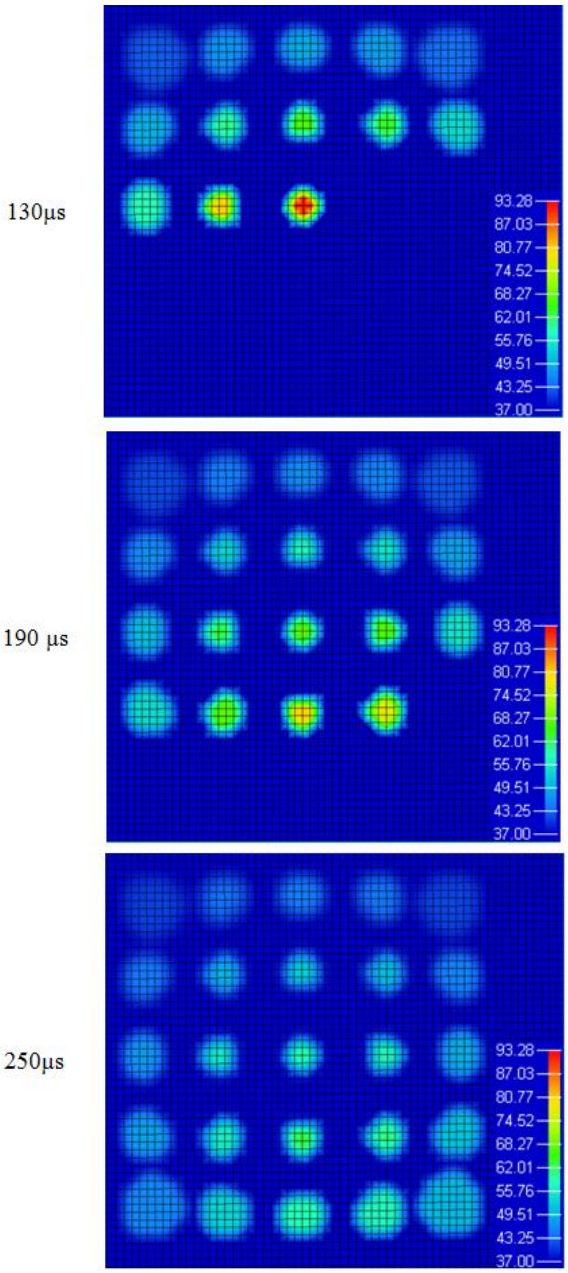

Figure 7. 61 diopters (Grid size = 10 µm / scaling in ℃)

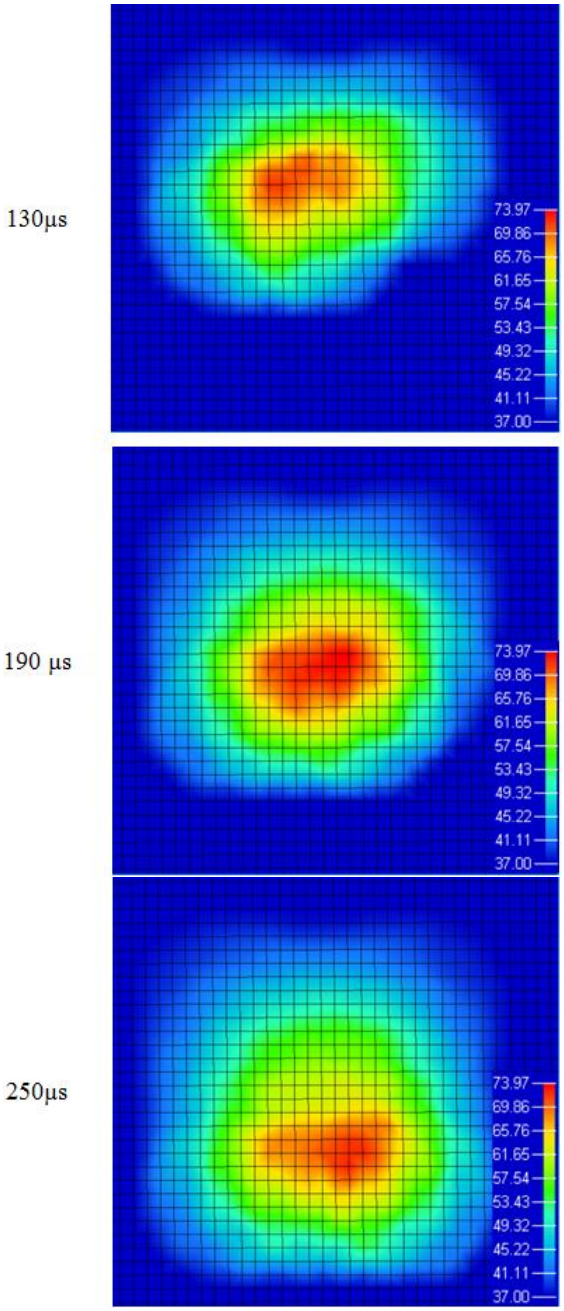

Figure 8. 67 diopters (Grid size = 10 µm / scaling in ℃)

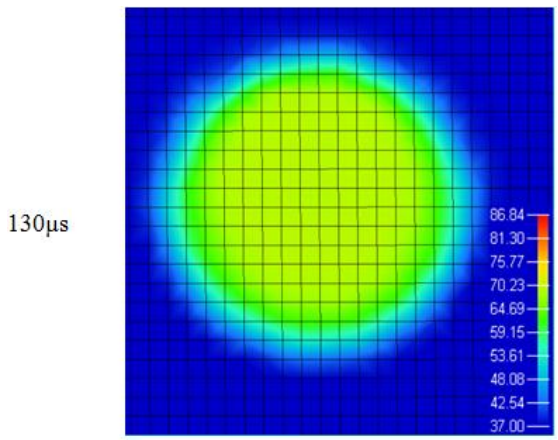

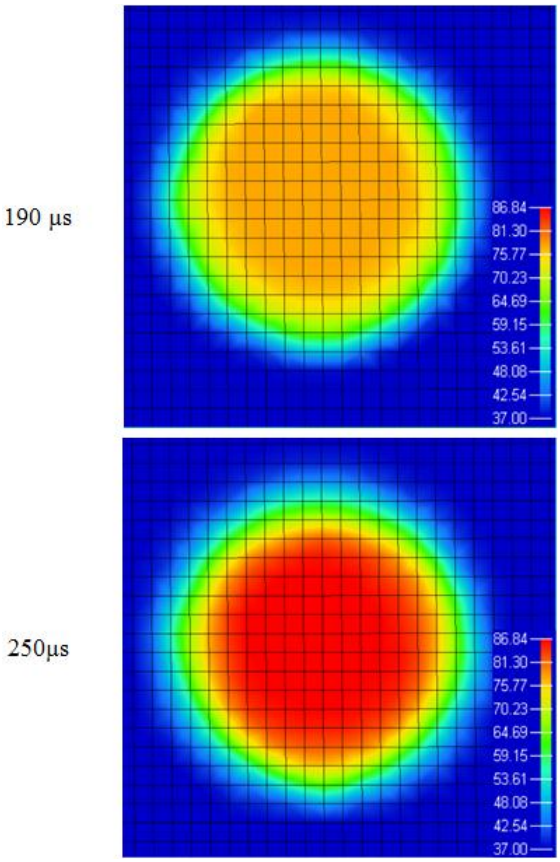

Figure 9. 71 diopters (Grid size = 10 µm / scaling in ℃)

The temporal developments of the retinal temperatures are plotted in Fig. 10. It shows how the point of highest temperature is changing over time. The small arrows indicate the point of damage, i.e. the point where the Arrhenius integral reaches a value of 1.

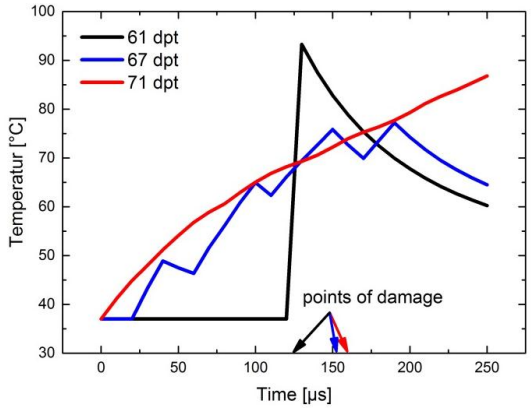

Figure 10. Temperature over time

Each curve reflects the behavior of the respective scanning pattern:

- An optical power of 61 diopters creates individual spots which do not affect each other, this explains the single peak. These spots are also smaller than in the other cases, this is the reason for the low point of damage: If the same amount of power is distributed over a smaller spot size the tissue is damaged faster.

- For 67 diopters a significant overlap occurs; the spots are affecting each other strongly as can be seen in Fig. 9. Therefore the temperature is increasing further whenever an overlapping spot is travelling over the hot spot and decreasing in the time before the next spot arrives.
- In the case of 71 diopters the spot positions are almost completely coincident which creates a constantly increasing temperature. The big spot diameter is the reason for the high point of damage.

Fig. 11 shows the development of the Arrhenius integral over time in comparison with the temperature for the case of 67 diopters. It demonstrates how fast the Arrhenius integral rises once the temperature is above 65 ℃ [11].

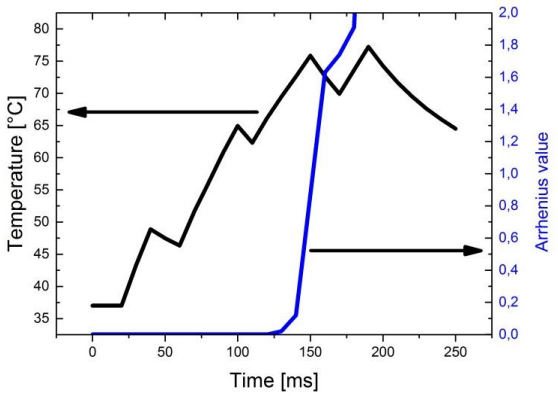

Figure 11. Temperature and value of the Arrhenius integral calculated for the case of 67 diopters

IV. Conclusion

We have demonstrated a complete tool chain which enables hazard predictions for different laser sources. Currently this model works in the regime of thermical damage, for the considerations of chemical and thermo-mechanical damage it needs to be extended.

V. Outlook

Even though the eye model which was used, has already been validated for non-scanning laser irradiation, the outcome of the presented calculations should be compared to respective scanning measurements to further improve the quality. We therefore aim for temperature and damage measurements implementing animal retinae.

Appendix - Warnings

Eye safety is a very complex issue and should be addressed by experts who evaluate optical designs before they are sold to the public.

An Arrhenius integral smaller than 1 does not necessarily mean that the calculated emission power satisfies the safety standards.

Acknowledgment

The authors would like to thank the Karlsruhe School of Optics and Photonics as well as the BMBF (Project Picolo, grant agreement number 13N12294) for funding and support. Special thanks go to Timo Nowak for his support during this work.

References

[1] N. Heussner, S. Bogatscher, S. Danilova, and W. Stork, "The impact of the revisions to the laser safety standard on the classification of scanned-beam projection systems," in *Proc. Int. Conf. Optics-Photonics Design & Fabrication*, Tokyo, 2014.

[2] N. Heussner, S. Bogatscher, and W. Stork, "Optimizing flying-spot display designs based on the upcoming edition of the laser safety standard," *Journal of the Society for Information Display*, 2014.

[3] S. Bogatscher, A. Streck, M. Fox, S. Meinzer, N. Heussner, and W. Stork, "Large aperture at low cost three-dimensional time-of-flight range sensor using scanning micromirrors and synchronous detector switching," *Applied Optics*, vol. 53, pp. 1570-1582, 2014.

[4] A. Frederiksen, R. Fie, W. Stork, S. Bogatscher, and N. Heussner, "Eye safety for scanning laser projection systems," *Biomed Tech*, vol. 57, pp. 175-184, 2012.

[5] R. H. Webb and G. W. Hughes, "Scanning laser ophthalmoscope," *IEEE Transactions on Biomedical Engineering*, vol. 28, no. 7, pp. 488-492, July 1982.

[6] E.-S. I and R. Navarro, "Off-axis aberrations of a wide-angle schematic eye model," *Journal of the Optical Society of America A*, vol. 16, no. 8, 1999.

[7] R. Henderson and K. Schulmeister, *Laser Safety*, New York: Taylor & Francis Group, 2004.

[8] N. Heussner, L. Holl, T. Nowak, T. Beuth, M. S. Spitzer, and W. Stork, "Prediction of temperature and damage in an irradiated human eye - Utilization of a detailed computer model which includes a vectorial blood stream in the choroid," *Computers in Biology and Medicine*, vol. 51, pp. 35-43, 2014.

[9] R. Brinkmann, S. Koinzer, K. Schlott, L. Ptaszynski, M. Bever, *et al.*, "Real-time temperature determination during retinal photocoagulation on patients," *Journal of Biomedical Optics*, vol. 6, 2012.

[10] E. Boettner and J. Wolter, "Transmission of the ocular media," *Investigative Ophthalmology & Visual Science*, vol. 6, pp. 776-783, 1962.

[11] M. Niemz, *Laser-Tissue Interactions*, 3 ed., Berlin Heidelberg: Springer, 2007.

[12] K. Schulmeister, B. Seiser, J. Husinsky, M. Jean, B. Fekete, and L. Farmer, "Damage thresholds for scanned exposure of the retina," in *Proc. International Laser Safety Conference*, Reno, 2009.

Nico Heussner studied electrical engineering with a focus on optical technologies at the Karlsruhe Institute of Technology (KIT) and the University of St. Andrews. After his graduation he joined the Institute for Information Processing Technology (ITIV) at the KIT as a member of scientific staff where he was working in the field of optical measurement techniques and laser-tissue-interaction. Since July 2012 he is continuing this work at the FZI – Forschungszentrum Informatik.

Wilhelm Stork received his Dipl.-Phys. degree by the University of Erlangen in 1984 and and the Dr. rer. nat. degree in optics in 1989 at the same university. He habilitated in electrical engineering in 2009 at the Karlsruhe Institute of Technology (KIT). From 1989 until 1993 he was organizing the Microsystems Division at the Institute for Optics at the University of Erlangen and became the Head of the Microsystems and Optics Division at the Institute of Information Processing Technologies (ITIV) at KIT in 1994. Since 2005 he has additionally been the Director of the Medical Information Technology Group at FZI in Karlsruhe before he became Professor of Electrical Engineering at ITIV in Karlsruhe.